Space Carving and Filtered Back-Projection as Preconditioners for Proton Computed Tomography Reconstruction

Blake Schultze[1], Micah Witt[1], Keith E. Schubert[1],[2], *Senior Member, IEEE*, Robert F. Hurley[3], Vladimir Bashkirov[3], *Member, IEEE*, Reinhard W. Schulte[2],[3] *Member, IEEE*, and Ernesto Gomez[1] *Member, IEEE*

***Abstract*—This paper considers how to determine the boundary of an object by comparing two methods: space carving (SC) and filtered back-projection (FBP). Determination of the boundary is an important first step in proton CT. The boundary is used to set up the large sparse linear system of equations, which are then solved to determine the relative stopping power of each element (voxel) in the object. For instance, to find the path of the proton through the object, the entry and exit points on the boundary must first be found. The boundary also becomes important in the iterative reconstruction, as only voxels inside the object are updated, to reduce computational complexity and prevent external artifacts from forming. SC and FBP are compared on speed and boundary results for four cases: (1) noiseless simulated data, (2) noisy simulated data, (3) a real pediatric head phantom, and (4) a real rat. The usefulness and potential of both methods are discussed and future directions are outlined.**

***Index Terms*—Proton Computed Tomography, Space Carving, Filtered Back-Projection, Preconditioning**

I. Introduction

PROTON computed tomography (pCT) predicts the range of proton beams in a patient more accurately than those from x-ray CT data. The pCT scanning data correspond to the water-equivalent path length (WEPL) of individual protons traversing the object from many different directions. Water-equivalent path length means that the proton would lose the same amount of energy by traversing this length in water rather than the object. Mathematically the WEPL can be expressed as the path integral of relative proton stopping power ($RSP = S_{mat}/S_{water}$) with respect to water, where $S = -dE/dx$, is the differential energy loss of protons per unit path length. Image reconstruction in pCT results in a 3D map of the relative stopping power (RSP), which is then used in proton treatment planning.

The reconstruction problem in pCT consists of solving a large and sparse linear system of equations of the form $Ax = b$, where the A-matrix contains the intersection lengths of the proton paths with the voxels of the reconstruction space, the b-vector contains the WEPL values, and the solution vector x contains the RSP value of each voxel after the system has been solved. However, this represents a circular problem: an accurate knowledge of A is needed to accurately reconstruct the object vector x, yet an accurate knowledge of x is needed to construct A in the first place [1]. Therefore, an accurate determination of the object hull is important for two reasons: it improves most likely path (MLP) calculations [2] used to produce A and preconditions the subsequent image reconstruction process [3].

Recent studies have demonstrated that pCT images of relatively high quality can be produced by performing iterative projection algorithms on a single GPU [4], [5], but reconstruction was too slow for practical use. Fortunately, the sparsity of the system matrix A and object vector x can be exploited to improve computational performance. However, the use of sparse matrices imposes new restrictions on hull-detection techniques. The most important of these new restrictions is that every voxel corresponding to a portion of the target object must be included in the object vector x. A sparse representation of x will contain only the voxels identified as belonging to the object. The remaining voxels, assumed to lie outside the object, are assigned an RSP of zero and do not enter into the reconstruction process. Therefore, these voxels are not updated during reconstruction and retain an RSP of zero in the final reconstructed image. The object hull should also contain as few voxels from outside the target object as possible. Maintaining unnecessary voxels reduces both the memory and computational benefits of using a sparse matrix format and slightly reduces the accuracy of the reconstructed image.

Although FBP has been an effective tool for determining an object hull in previous work [4], [5], several concerns have arisen that call its continued use into question. An image reconstruction technique like FBP appears excessively complex for simply identifying the bounds of an object, which may be possible with less effort. FBP for pCT reconstruction requires spatial binning of the proton histories, and results

Manuscript received November 15, 2012. This work is supported by Grant No. 1R01EB013118-01 from the Institute of Biomedical Imaging and Bioengineering at the National Institutes of Health and the National Science Foundation. The content of this paper is solely the responsibility of the authors and does not necessarily represent the official views of the National Institute of Biomedical Imaging and Bioengineering or the National Institutes of Health. Reinhard Schulte is supported by the United States - Israel Binational Science Foundation (BSF), grant Number 2009012.1

[1] Blake Schultze, Micah Witt, Ernesto Gomez and Keith Schubert are with the School of Computer Science and Engineering, California State University San Bernardino, San Bernardino CA 92407 USA, email: blake@r2labs.org

[2] Keith Schubert and Reinhard Schulte are with the Department of Basic Sciences, Loma Linda University Medical Center, Loma Linda CA 92354 USA

[3] Reinhard Schulte, Vladimir Bashkirov, and Robert F. Hurley are with the Department of Radiation Medicine, Loma Linda University Medical Center, Loma Linda CA 92354 USA, email: rschulte@dominion.llumc.edu

of this binning process, e.g., mean and standard deviations of the WEPL values in each bin can be exploited to exclude spurious events related to inelastic nuclear interactions. If these intermediate results are no longer necessary, they become computationally expensive calculations used exclusively for FBP. While these concerns are purely performance related, FBP may also be incapable of satisfying the aforementioned restrictions imposed by sparse matrix reconstruction techniques. As a result, a hull-detection technique has been introduced which may provide an accurate and computationally efficient alternative to FBP for preconditioning sparse matrix reconstruction.

Unfortunately, it is difficult to predict the impact the accuracy of the object hull on the quality of the final reconstructed image, as the convergence properties of iterative reconstruction algorithms varies with the accuracy of the initial iterate. Since the relationship between the accuracy of the object vector and computational performance have not been determined, reconstructed images were not considered in this paper. Therefore, the goal of this work was to evaluate the suitability of space carving (SC), which determines the voxels of the reconstruction volume that lie outside the boundary of the scanned object using proton histories that entirely avoid it, and compare this to conventional (2D or 3D) FBP used previously. In particular, computation time and the quality of the object hull determined for a digital head phantom, a pediatric head phantom, and a live rat under anesthesia were determined for each technique.

II. Methods

In an effort to reduce resource needs and improve performance and accuracy, many of the preprocessing and image reconstruction techniques are being revisited to identify inefficiencies and develop alternatives. Object hull-detection is perhaps the most important aspect of preprocessing as this directly impacts the quality of the reconstructed images and the speed at which convergence occurs. FBP had already been identified as an overly complex hull-detection technique, but it now appears it may also be an unsuitable technique for sparse matrix reconstruction, thereby increasing the appeal of developing an alternative method which can satisfy the new preconditioner restrictions.

The specific aim of a hull-detection technique is to simply identify which voxels belong to the object and which do not. Much of the information elicited by FBP is irrelevant to this classification and the desired information can only be inferred from its use. FBP reconstructs explicit RSP values for each voxel and makes no direct determination of whether or not a voxel belongs to the target object, this determination must be made based on RSP values. On the other hand, SC was developed specifically and exclusively for this purpose and is thus considerably less complex and more efficient. Whereas FBP attempts to construct the object hull by determining all the voxels which belong to it, SC takes the inverse approach, determining which voxels do not belong to the object and removing them from consideration to reveal the hull. Although SC remains in preliminary development, it represents a particularly appealing alternative to FBP for several reasons.

A. Space Carving (SC)

Space carving (SC) is a simple and computationally inexpensive hull-detection technique analogous to the way a sculptor chisels away undesired portions of a block of material to produce a sculpture [6], [7], [8]. In this case, the block of material is the entire cylindrical reconstruction volume and the portions being chiseled away are defined by the proton paths that miss the target object. If a proton does not pass through the object being scanned, it will experience an insignificant amount of scattering. Therefore, the measurements obtained for protons that pass exclusively through air will have the smallest WEPL variance and are theoretically the most accurate measurements obtained in a scan. The limited energy loss can then presumably be used to identify which protons missed the object and the voxels it passed through can be removed from the object vector x. Figure 1 shows the process by which a proton path (blue) is used to exclude voxels (red) from the object vector (the remaining voxels shown in green).

Repeating this for every proton that missed the object, all of the voxels outside the object will have been identified and removed. It can be assumed that the remaining voxels contain at least some portion of the object, so that collectively, they represent an approximate definition of the object and its boundaries. For this work, a WEPL value of 1.0 mm was used to discern between protons that passed through the object and those that did not. If a proton yielded a WEPL$\leq$1.0 mm, it was assumed to have missed the object entirely and the voxels along its path, the line connecting the points where the proton entered and exited the reconstruction volume, were carved from the reconstruction cylinder.

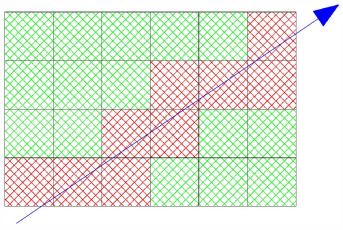

Fig. 1. Using the path of the proton (blue) to exclude voxels (red) from the object vector (green)

B. Filtered Back-Projection (FBP)

Filtered back-projection is an image reconstruction technique that has been used in recent work to determine an approximate object hull for use in MLP calculations and as the initial iterate in subsequent image reconstruction [2], [3], [4], [5]. FBP accounts for statistical variations in WEPL measurements by determining the mean WEPL value for protons that followed similar paths and then uses this to remove spurious events from consideration. Combining measurements from numerous angles produces a sinogram from which an approximate RSP is calculated for each voxel. The three-dimensional cone-beam analogue of FBP, known as the Feldkamp Davis Kress (FDK) algorithm [9], was used for this work which assumes each proton follows a straight-line path. The angular bins were 4° wide, lateral bins were 0.1 cm wide,

vertical bins were 0.5 cm wide, and the Shepp-Logan filter was used prior to back-projection. The reconstruction volume was a 9.6 cm tall cylinder with a 10 cm radius and each slice was 20 cm wide $\times$ 20 cm high $\times$ 0.3 cm thick, producing a total of 9.6 cm/0.3 cm = 32 slices. To determine an approximate object hull, a threshold WEPL value of 0.6 was used to determine which voxels are likely part of the object and which are not. If a voxel has an RSP$\geq$0.6, the voxel is assumed to be part of the object and is assigned an RSP of 1; if a voxel has an RSP$<$0.6, the voxel is assumed to lie outside the object boundary and is assigned an RSP of 0.

III. Input Data

Fig. 2. Digital head phantom used to produce the two simulated data sets

Two types of data were used in this work to evaluate the hull-detection techniques: simulated data and experimental data. Two data sets (11,796,480 proton histories each) were produced by simulating random proton paths through the digital head phantom in Figure 2 [10]. The first data set summed the RSP values of voxels along the path of a proton to produce a noiseless WEPL value for each proton history. The second data set added a noise component to the corresponding noiseless WEPL value, calculated based on the standard deviation in energy expected from Tschalar's energy straggling theory [11].

The two experimental data sets were acquired using the proton accelerator at Loma Linda University Medical Center. One data set contains 50,897,953 proton histories obtained from a scan of a anthropomorphic pediatric head phantom, Model 715-HN, CIRS; the second data set contains 65,128,961 proton histories obtained from a scan of a living rat held in restraints and under anesthesia.

IV. Results

Figure 3 shows the object hulls obtained from each data set using SC (top row) and FBP (bottom row) and the corresponding computation times are shown in Table I. Notice that the simulated data results for SC are quite impressive and were obtained nearly 1000 times faster than those from FBP. These results also show that SC was insensitive to noise, while the quality of the FBP results declined considerably with the introduction of noise. Another issue with the FBP results is that the RSP value of some voxels from the interior of the object fell below the threshold and were not included in the object vector x. In addition, numerous voxels lying outside the object were included in x, more prevalently with the introduction of noise. This sensitivity to noise is alarming as noise is an unavoidable reality of experimental data.

Streaks are commonly introduced as a result of the back-projection process, as energy loss is assumed to have happened smoothly along each proton path, including voxels outside the object since its boundaries are unknown at this point. Since the amount of energy deposited in voxels outside the object is then overestimated, the amount of energy deposited in voxels in the interior of the object, and therefore their RSP value, is underestimated. These unnecessary voxels in the object vector x are therefore maintained throughout the reconstruction process, thereby increasing memory usage and computation time as well as slightly reducing the accuracy of the reconstructed image.

On the other hand, the results obtained with SC using the experimental data (pediatric head phantom and live rat), although still about 1000 times faster than FBP, show that a significant number of voxels belonging to the target object were mistakenly excluded from the object hull. Clearly there were several protons passing through the interior of the object which were identified as having missed the object entirely, resulting in the removal of several lines of voxels through the object. Despite the infrequency of the spurious events causing these voxels to be invalidly removed from the object, with tens of millions of proton histories, it was enough to carve several paths from the interior of the object.

TABLE I
Computation Times

	FBP	SC
Simulated: Noiseless	16.695 s	$<$100 ms
Simulated: Noisy	16.723 s	$<$100 ms
Pediatric Head	18.872 s	$<$100 ms
Rat	19.912 s	$<$100 ms

V. Summary and Discussion

Although this work was preliminary in nature, several insights can be gleaned from the results obtained. One aspect of SC that makes it a particulary appealing preconditioning technique is its simplicity and computational efficiency, consistently producing results nearly 1000 times faster than FBP. In fact, the 100 ms reported for SC is an extremely conservative estimate since nearly all of the 90 separately processed projection angles exceeded the millisecond precision of the program timer. However, efforts were not made to establish an exact computation time because an inflated approximation does not detract from the impressive performance relative to FBP. The simulated data results obtained with SC, both with and without noise, establish its theoretical efficacy and considerable potential. SC results demonstrated an insignificant sensitivity to noise which it derives from exclusive use of protons passing entirely through air, as these are the most accurate measurements collected. On the other hand, the quality of the FBP results deteriorated appreciably with the addition of noise since FBP also uses proton histories

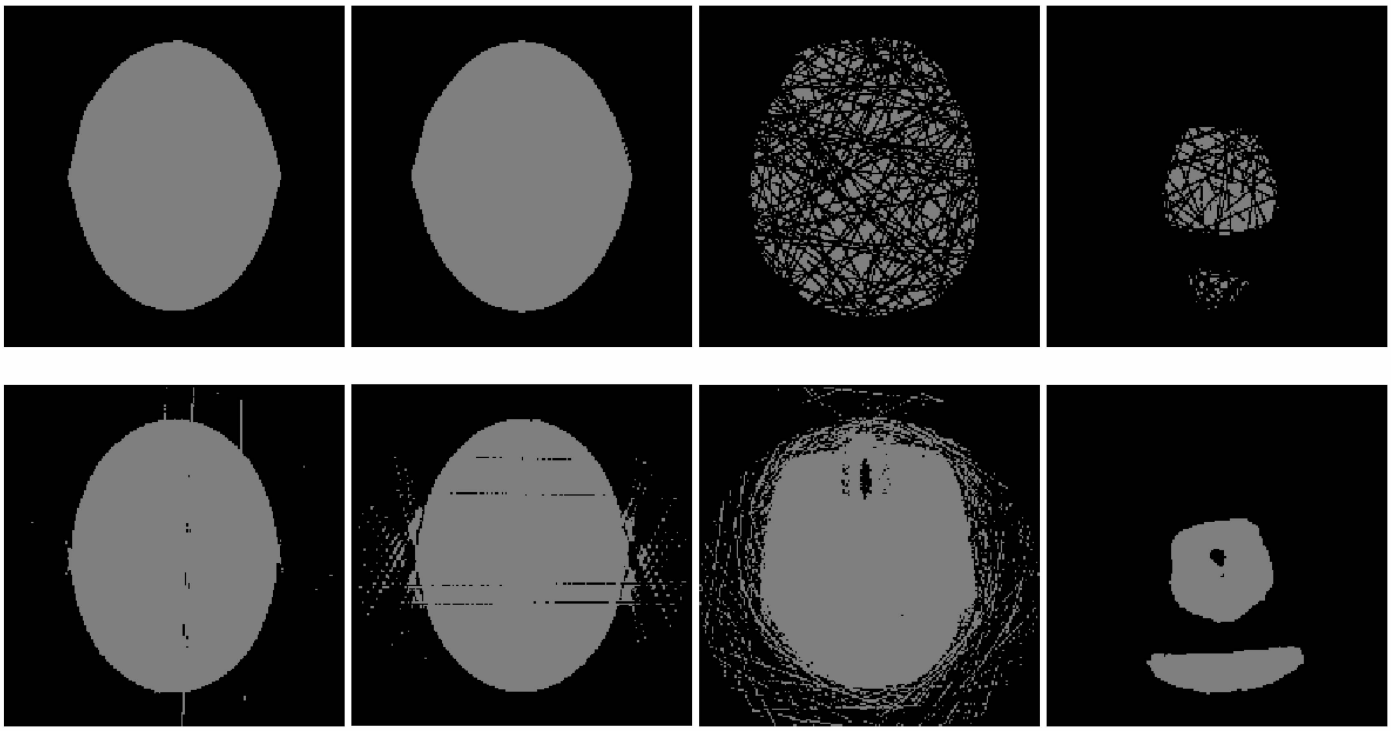

(a) Noiseless Simulated Data (b) Noisy Simulated Data (c) Pediatric Head Phantom (d) Rat

Fig. 3. The object hulls determined by SC (top row) and FBP (bottom row) for each of the data sets

yielding larger WEPL measurements, which inherently contain more noise.

In addition, SC did not exclude any of the voxels from the interior of the target object using either of the simulated data sets, while FBP produced an object hull with several voxels missing from the interior. Unfortunately, close inspection revealed that both techniques missed voxels from the perimeter of the digital head phantom. These missing voxels can theoretically be added, provided the object boundary can be determined accurately. However, the voxels lying sporadically outside the object hull found with FBP makes determining the boundary of the object challenging, particularly with the pediatric head phantom. On the other hand, adding an appropriately large layer of voxels to the object hull found using SC can be accomplished quite easily, but the removal of these voxels may be avoidable in the first place.

Despite the fact that simulated data is an extremely useful tool for confirming the theoretical feasibility of a technique or algorithm, the ultimate test of applicability is its performance in a realistic setting. The speed at which SC performed remained consistent with the considerably larger experimental data sets, but the object hull rendered for the pediatric head phantom and the live rat were both unsatisfactory. Although infrequent (only a fraction of a percent of the time), spurious histories, most likely the effect of multiple proton events, caused significant portions of the target object to be excluded from the object vector x. The proton accelerator typically ejects a single proton at a time, but on rare occasions (according to a Poisson PDF), two protons are simultaneously launched towards the target. When this occurs, several issues can arise which may affect downstream measurements.

Two pairs of Single-Sided Strip Detectors (SSDs), one pair on each side of the object being scanned, are used to determine the position and trajectory of the proton before and after the target. When two protons pass through the SSDs simultaneously, there are two intersection points recorded by each detector plane, making it difficult to determine which of the two intersection points belong to a particular proton. If a SSD intersection point is assigned to the wrong proton, the paths calculated for both protons will be erroneous. This can lead to, for example, the assumption that a proton missed the object when it actually passed through it. This type of an event is consistent with the observed behavior.

However, the more insidious and far more likely explanation for the observed complications is the effect of "pile-up" in the energy detector. When a proton hits the energy detector (in this case, CsI calorimeter), the response is measured and later converted into an approximate WEPL value. Unfortunately, the detector response does not return to null-input level immediately, it decays at a rate depending primarily on the capacitive and inductive properties of both the detector and readout electronics and what might be called "after glow", which photodiodes detect until all ionized atoms decay. Therefore, when two protons enter the calorimeter, separated in time by less than the time it takes the detector response to decay, whatever residual signal remains is added to the response from the second proton, thereby inflating the detector response. This inflated response results in a reduced WEPL measurement, potentially causing a proton that passed through the object to appear as if it did not.

The raw data supports this explanation, both qualitatively and quantitatively. Qualitatively, this explains the lines re-

moved from the object hull. Quantitatively, this type of erroneous data would skew measurements towards unexpectedly low WEPL values, which was also observed. WEPL measurements for a proton that missed the object are typically 1-2 mm but can also be slightly negative. However, numerous WEPL measurements in the experimental data are less than -2 mm, which can happen, but not with the frequency observed. These large negative WEPL values imply that protons entering the calorimeter have more energy than they did exiting the accelerator. Although the energy of protons leaving the accelerator varies, this does not appear to be a sufficient or likely cause for the observed events.

Prior to determining that pile-up was the likely cause of the observed problems, the SC results were significantly worse. Initially, any proton history with a WEPL$<$1.0 mm was assumed to have passed entirely through air. The result was the exclusion of every single voxel from the object hull, producing a completely blank image. The WEPL threshold had to be lowered to -2.5 mm to retain any voxels, but at this level, the voxels that remained appeared completely random. Assuming that the large negative WEPL values were the result of pile-up, for analysis purposes, a proton path was carved from the object only if 0.0 mm$\leq$WEPL$\leq$1.0 mm. The images in Figure 3 from the experimental data show the result of the modified thresholding procedure. The dramatic improvement strengthens the argument that misidentified proton histories were attributable to pile-up. Aside from the few remaining lines of voxels removed from the interior of the objects, their boundaries were determined reasonably accurately. Although this does not represent an ideal solution to the problem, as any WEPL range will likely contain pile-up events, the missing portion of the objects could be filled in reasonably easily.

Since SC is considerably faster than FBP, additional calculations can likely be introduced to overcome the aforementioned pile-up error while still computationally outperforming FBP. One possible solution is to add a threshold to the relative angle of the proton, that is, the difference between the proton angle passing through the first set of SSDs and the angle passing through the second set of SSDs. As mentioned, when a proton passes through nothing but air, it will experience insignificant scattering, resulting in limited angular deviation. Therefore, the relative angle for protons that miss the object should be smaller than those that pass through it. However, since the relative angles are small for all proton histories, especially with the rat data because of its size, the histories may be difficult to discern based on relative angle. In this case, protons that did miss the object but scattered more than usual will occasionally be ignore as well. In addition, some erroneous events may satisfy the thresholds and still cut out part of the object. A balance would have to be found which cuts out the troublesome events and retains enough of the proton histories that missed the object to adequately carve the object hull. A far more likely solution is to not exclude a voxel from the object vector after the first time it's identified as lying outside the object but to instead implement some more sophisticated technique which also considers the number of times. On the other hand, the ideal solution would be to remove events with multiple protons at the detector and as they occur.

While the results using FBP on the experimental data were not nearly as poor as those obtained using SC, FBP presented similar issues with the experimental data as it did with the simulated data. In addition to FBP being computationally expensive, the thresholding process used to determine the object boundary introduces holes into the object interior, as can be seen in every image in Figure 3, most notably the sinus region of the pediatric head phantom. The streaks of additional voxels lying outside the object boundary compound the issue, as their presence makes finding the object boundary difficult and prevents the missing voxels from being easily identified and filled in. Since the issues encountered with FBP do not appear to have an immediately obvious or straightforward solution, an alternative preconditioning technique should be developed that can satisfy the criteria arising from the use of sparse matrices.

SC is an attractive preconditioning technique due to its simplicity and computational efficiency. Considerable promise has been demonstrated in this work but the issues encountered with experimental data, most likely the result of pile-up, must be addressed. As data acquisition is being improved in parallel with data processing and image reconstruction, issues such as pile-up may be avoidable in the future. Until such time, however, preconditioning development will focus on alleviating the effect of these issues and improving the speed and accuracy of hull-detection. Several possible solutions have been suggested here and will be investigated in future work, along with alternative preconditioning techniques. Once multiple viable preconditioning techniques have been developed, studies into the required accuracy of object matrices and the relationship between their accuracy and performance will be performed to aid final selection.

REFERENCES

[1] S. N. Penfold, R. W. Schulte, Y. Censor, V. Bashkirov, S. Macallister, K. E. Schubert, and A. B. Rosenfeld, "Block-iterative and string-averaging projection algorithms in proton computed tomography image reconstruction," in *Biomedical Mathematics: Promising Directions in Imaging, Therapy Planning and Inverse Problems*, Y. Censor, M. Jiang, and G. Wang, Eds., The Huangguoshu International Interdisciplinary Conference. Madison, WI, USA: Medical Physics Publishing, 2010.

[2] R. Schulte, S. Penfold, J. Tafas, and K. Schubert, "A maximum likelihood proton path formalism for application in proton computed tomography," *Journal of Medical Physics*, vol. 35, no. 11, pp. 4849–4856, November 2008.

[3] S. N. Penfold, A. B. Rosenfeld, R. W. Schulte, and K. E. Schubert, "A more accurate reconstruction system matrix for quantitative proton computed tomography," *Journal of Medical Physics*, vol. 36, no. 10, pp. 4511–4518, October 2009.

[4] S. Penfold, "Image reconstruction and monte carlo simulations in the development of proton computed tomography for applications in proton radiation therapy," Ph.D. dissertation, University of Wollongong, Australia, 2010.

[5] S. Penfold, R. Schulte, Y. Censor, and A. Rosenfeld, "Total variation superiorization schemes in proton computed tomography image reconstruction," *Med Phys*, vol. 37, pp. 5887–5895, 2010.

[6] K. N. Kutulakos and S. M. Seitz, "A theory of shape by space carving," in *Proc. Seventh International Conference on Computer Vision (ICCV)*, 1999, pp. 307–314.

[7] ——, "A theory of shape by space carving," *International Journal of Computer Vision*, vol. 38, no. 3, pp. 199–218, Marr Prize Special Issue 2000.

[8] S. S. S. Vedula, S. Baker and T. Kanade, "Shape and motion carving in 6d," in *Proc. Computer Vision and Pattern Recognition Conf. (CVPR)*, 2000.

[9] K. J. Feldkamp LA, Davis LC, "Practical cone-beam algorithms," *J Opt Soc Am A*, vol. 6, pp. 612–619, 1984.
[10] M. Witt, R. Schulte, and K. Schubert, "A proton simulator for testing implementations of proton ct reconstruction algorithms on gpgpu clusters," in *Proceedings of the IEEE Nuclear Science Symposium Medical Imaging Conference*, 2012.
[11] C. Tschalar, "Straggling distributions of extremely large energy losses," *Nuclear Instruments and Methods*, vol. 61, p. 141156, 1968.